Supplementary Material

1 Optimum Multiparameter (OMP) Analysis

The optimum multi-parameter (OMP) analysis by (Karstensen and Tomczak, 1999) was used to quantify the relative contributions of different water masses from the samples collected during the TransArc II expedition to the Arctic Ocean with the German R/V Polarstern (PS94, ARK-XXIX/3, Tromsø-Tromsø) in the framework of the international GEOTRACES program (GEOTRACES transect GN04). The OMP analysis is a set of n linear equations from observations of n+1 parameters determined and an equation for mass conservation (Tomczak, 1981). The contribution of the n water masses to a given water sample gives the exact solution to the n equations (Tomczak, 1981). The set of linear equations are solved in order to have the best fit for x fraction of n water masses to the n+1 observed parameter to minimize the residual error. In order to perform the OMP analysis we used the MATLAB code by (Karstensen and Tomczak, 1999) openly available on https://omp.geomar.de/node3.html.

The water mass definitions by Rudels et al. (2012) were used to characterize the different water masses in our study area. In total, six water masses were used in this study. The World Ocean Atlas (WOA-2013) was used to determine the possible endmember values for the parameters used in our OMP analysis. The parameters used were: salinity (Zweng et al., 2013), potential temperature (Locarnini et al., 2013), and oxygen (Garcia et al., 2014a), silicate, nitrate and phosphate concentrations (Garcia et al., 2014b). In order to define the endmembers, a section was determined, using ODV, which is located upstream along the flow path of the waters of the transect of our study area in the Central Arctic Ocean (Fig. S1, Fig. 1). At this section, 4-6 data points each for oxygen, silicate, nitrate and phosphate concentrations were retrieved from WOA 2013 that were within the complete range of temperature, salinity and density determined for each water mass by Rudels et al. (2012) (Fig. S1). From these 4-6 values, an average value was calculated along with its variance, which then was used as the end member for each water mass. This method of retrieving data from WOA was previously used for OMP analysis with satisfactory results in a study in the Pacific Ocean (Behrens et al., 2018), therefore we chose the same method. Additionally, the availability of data from WOA made possible the determination of the endmember waters prior the transect in the Arctic Ocean without influence that the samples could have been suffering. The weighting for the different parameters were determined by the square of the standard deviation of all water masses divided by the highest variance of the parameter (Table S1). This is done in order to make the parameters of incommensurable units comparable (Karstensen and Tomczak, 1999). The OMP results are shown in Figure 3.

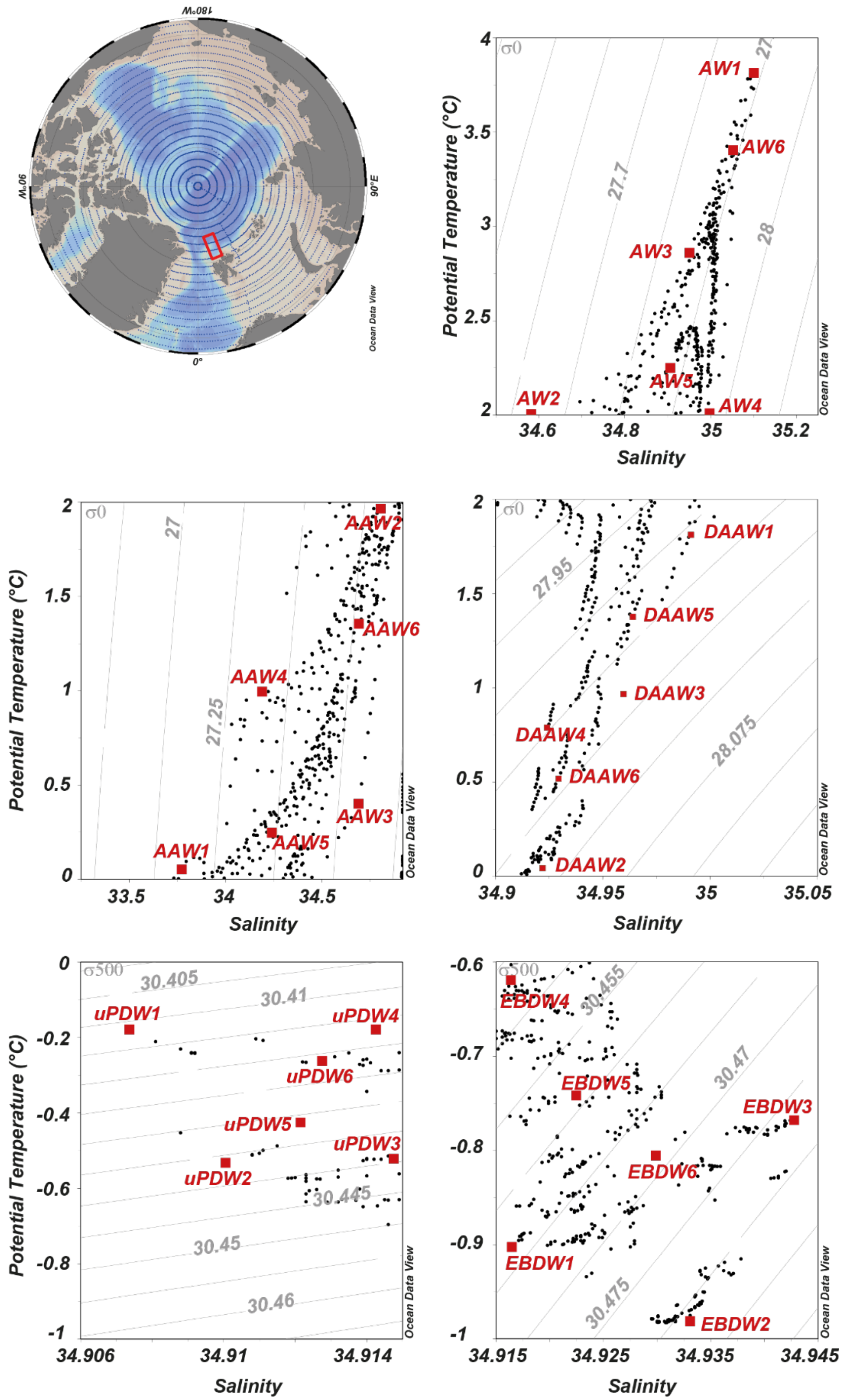

Supplementary Figure 1. Section used to determine endmember composition of the parameters for OMP analysis, using ODV and WOA-13 data. In red are the stations/depths highlighted that were used to calculate average values for each water mass. The stations were chosen within the section band upstream of the stations used for δ^{30}Si-DSi determinations. The endmembers were defined based on previous water masses definitions (Rudels et al., 2012), where the different parameters retrieved from the WOA from each station were chosen within the range of water mass definitions.

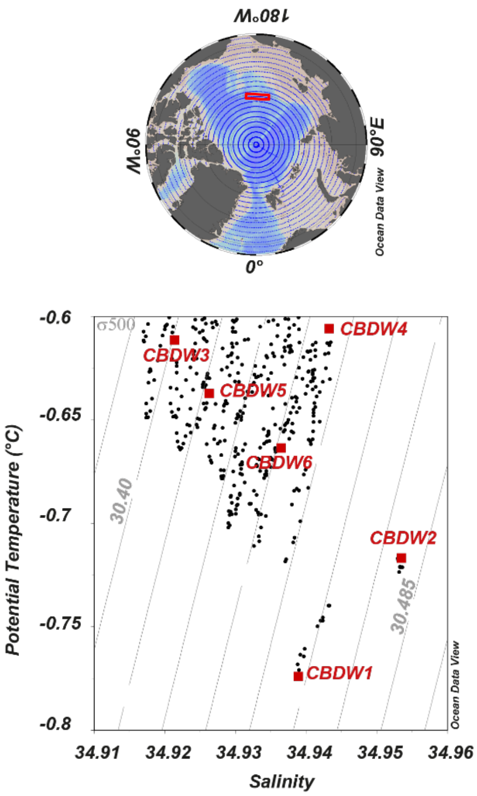

Supplementary Figure 1. Continuation

Supplementary Table 1: Water masses definitions and weights used for OMP analysis.

	AW	AAW	DAAW	uPDW	EBDW	CBDW	Weights
Potential temp. θ (°C)	2.87	0.84	0.92	-0.35	-0.87	-0.67	1.98
Salinity	35.01	34.39	34.95	34.91	34.93	34.94	0.27
Oxygen (µmol L^{-1})	314.72	340.23	314.65	309.41	310.04	291.75	0.96
Phosphate (µmol L^{-1})	0.79	0.61	0.91	0.94	0.99	1.07	3.10
Nitrate (µmol L^{-1})	11.47	7.30	13.48	13.89	15.03	15.01	1.16
Silicate (µmol L^{-1})	5.98	5.28	7.00	8.60	11.68	13.28	2.10

2 Data Quality

Supplementary Figure 2 implies that samples from the Eurasian Basin of the AO have, on average, lower δ^{30}Si-DSi compared to samples from the North Atlantic (de Souza et al., 2012) or the Canadian Basin of the AO (Varela et al., 2016), which can be partly explained by inter-laboratory offsets that have been acknowledged before (Grasse et al., 2017) (see also main text). However, as shown in Supplementary Figure 3, our low concentrated seawater samples show a slight offset for the δ^{30}Si-DSi values from the mass-dependent fractionation line towards lighter than expected values (we assume that the δ^{29}Si values are generally more reliable because the measurements are much less affected by potential isobaric interferences). This is most likely related to the effects of high matrix:DSi ratios in the low DSi concentrated seawater samples. It has been suggested before that the Neptune MC-ICP-MS is more affected by remaining matrix in the samples than e.g. the NU Plasma MC-ICP-MS, which could be the reason for these effects. However, most samples are, within error, within the range of the theoretical mass dependent fractionation line.

To still acknowledge this, we do not discuss any variations in the data set that can be seen only in one or few samples, but instead focus on general variations in δ^{30}Si of the main water masses in the Central Arctic Ocean (Atlantic Water - AW, Dense Arctic Atlantic Water - DAAW, Upper Polar Deep Water - uPDW, Eurasian Basin Deep Water - EBDW and Canadian Basin Deep Water - CBDW). For this, we calculated mean δ^{30}Si-DSi for each water mass, which is defined through OMP analysis, and then compare and discuss only deviations of these mean values from each other. The mean values for each water mass are based on a number of individual data points: AW n = 3, DAAW n = 22, uPDW n = 12, EBDW n = 25 and CBDW n = 7. The relative offset between those average values within our data set is not affected by the uncertainty of the measurements. We also calculated average values for the water masses based on the δ^{29}Si-DSi as well as theoretical δ^{30}Si-DSi (=δ^{29}Si-DSi/0.51) (Supplementary Figure 4). Obviously, the general pattern is the same, independent of which isotope ratio is used, supporting our interpretation of the data.

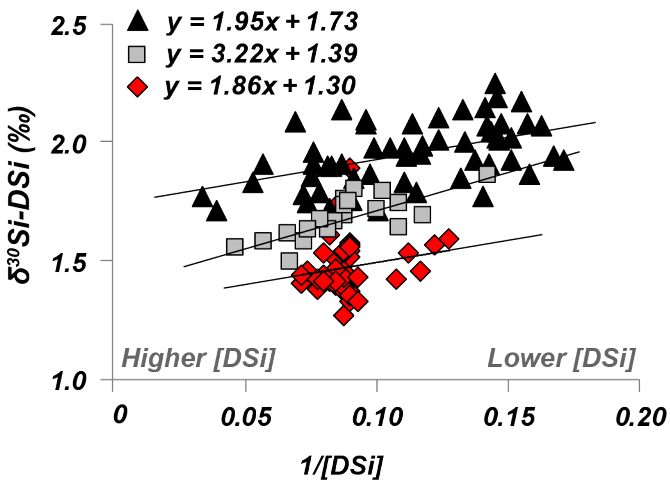

Supplementary Figure 2 δ^{30}Si-DSi *versus* the inverse of [DSi] for waters >1000 m water depth from the Eurasian Basin (this study, red diamonds), the Canadian Basin (Varela et al., 2016, black triangles) and the North Atlantic (de Souza et al., 2012, grey squares). Equations reported refer to the linear regressions produced for each dataset.

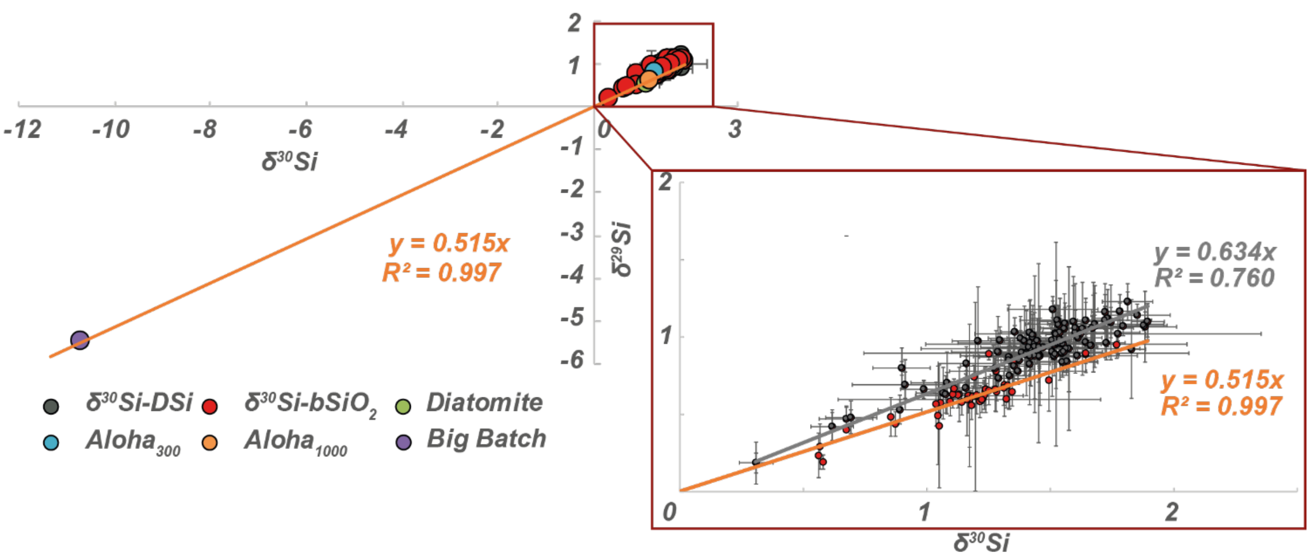

Supplementary Figure 3 Cross plot for δ^{30}Si/δ^{29}Si (in ‰) from all samples and standards (Big Batch and Diatomite). The determined slope of 0.515 (represented by the orange trend line) shows that the Si isotopes follows a mass-dependent fractionation, close to the kinetic fractionation value for Si isotopes (0.5092), see also Reynolds et al. (2007). Grey trend line represents the slope for all samples (0.634), without standards.

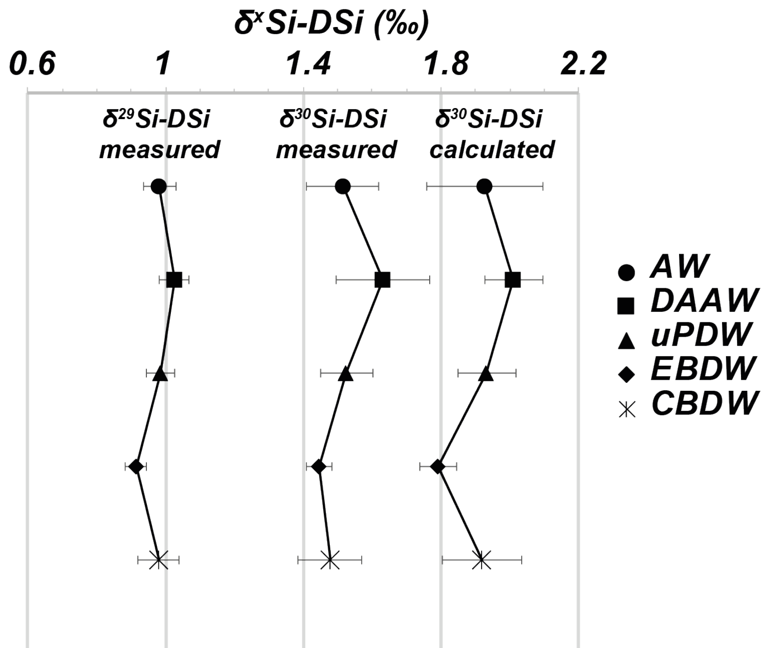

Supplementary Figure 4 Comparison between average δ^{29}Si-DSi (measured), δ^{30}Si-DSi (measured) and theoretical calculated δ^{30}Si-DSi (=δ^{29}Si-DSi$_{measured}$/0.51) for each water mass. Error bars represent 2SEM.

References

De Souza, G. F., Reynolds, B. C., Rickli, J., Frank, M., Saito, M. A., Gerringa, L. J., & Bourdon, B. (2012). Southern Ocean control of silicon stable isotope distribution in the deep Atlantic Ocean. *Global Biogeochemical Cycles*, *26*(2).

Garcia, H. E., R. A. Locarnini, T. P. Boyer, J. I. Antonov, O.K. Baranova, M.M. Zweng, J.R. Reagan, D.R. Johnson, 2014a. World Ocean Atlas 2013, Volume 3: Dissolved Oxygen, Apparent Oxygen Utilization, and Oxygen Saturation. S. Levitus, Ed., A. Mishonov Technical Ed.; NOAA Atlas NESDIS 75, 27 pp.

Garcia, H. E., R. A. Locarnini, T. P. Boyer, J. I. Antonov, O.K. Baranova, M.M. Zweng, J.R. Reagan, D.R. Johnson, 2014b. World Ocean Atlas 2013, Volume 4: Dissolved Inorganic Nutrients (phosphate, nitrate, silicate). S. Levitus, Ed., A. Mishonov Technical Ed.; NOAA Atlas NESDIS 76, 25 pp.

Karstensen, J., & Tomczak, M. (1999). Manual for OMP Analysis Package for MATLAB, version 2.0. Retrieved from https://omp.geomar.de/node3.html

Locarnini, R. A., A. V. Mishonov, J. I. Antonov, T. P. Boyer, H. E. Garcia, O. K. Baranova, M. M. Zweng, C. R. Paver, J. R. Reagan, D. R. Johnson, M. Hamilton, and D. Seidov, 2013. World Ocean Atlas 2013, Volume 1: Temperature. S. Levitus, Ed., A. Mishonov Technical Ed.; NOAA Atlas NESDIS 73, 40 pp.

Reynolds, B.C., Aggarwal, J., Andre, L., Baxter, D., Beucher, C., Brzezinski, M.A., Engström, E., Georg, R.B., Land, M., Leng, M.J. & Opfergelt, S. (2007). An inter-laboratory comparison of Si isotope reference materials. *Journal of Analytical Atomic Spectrometry*, *22*(5), 561-568.

Rudels, B., Anderson, L., Eriksson, P., Fahrbach, E., Jakobsson, M., Jones, E. P., Melling, H., Prinsenberg, S., Schauer, U. & Yao, T. (2012). Observations in the ocean. In *Arctic Climate Change* (pp. 117-198). Springer, Dordrecht.

Tomczak Jr, M. (1981). A multi-parameter extension of temperature/salinity diagram techniques for the analysis of non-isopycnal mixing. *Progress in Oceanography*, *10*(3), 147-171.

Varela, D. E., Brzezinski, M. A., Beucher, C. P., Jones, J. L., Giesbrecht, K. E., Lansard, B., & Mucci, A. (2016). Heavy silicon isotopic composition of silicic acid and biogenic silica in Arctic waters over the Beaufort shelf and the Canada Basin. *Global Biogeochemical Cycles*, *30*(6), 804-824.

Zweng, M.M, J.R. Reagan, J.I. Antonov, R.A. Locarnini, A.V. Mishonov, T.P. Boyer, H.E. Garcia, O.K. Baranova, D.R. Johnson, D.Seidov, M.M. Biddle, 2013. World Ocean Atlas 2013, Volume 2: Salinity. S. Levitus, Ed., A. Mishonov Technical Ed.; NOAA Atlas NESDIS 74, 39 pp.